

Electrochemical Impedance Spectroscopy of Sandy Soil Containing Cl^- , SO_4^{2-} and HCO_3^-

Ruizhen Xie^{1,*}, Yating Xie¹, Boqiong Li¹, Pengju Han^{2*}, Bin He², Baojie Dou³, Xiaohong Bai²

¹ Department of Materials Science and Engineering, Jinzhong University, Jinzhong 030619, China

² Department of Civil Engineering, Taiyuan University of Technology, Taiyuan 030024, China

³ Material Corrosion and Protection Key Laboratory of Sichuan province, Sichuan University of Science and Engineering, Zigong 643002, China

*E-mail: 13834569544@163.com, 18735394929@163.com

Received: 14 August 2021 / Accepted: 17 October 2021 / Published: 10 November 2021

Based on orthogonal experiments, electrochemical impedance spectroscopy was used to study the characteristics of sandy soils containing Cl^- , SO_4^{2-} and HCO_3^- , and the universality of the equivalent circuit was also studied. The influence of Cl^- , SO_4^{2-} and HCO_3^- on the electrochemical behavior and corrosivity of sandy soil was studied by range analysis. The results show that the Nyquist diagrams of sandy soils all present capacitive reactance arcs in the high-frequency region and different diffusion slopes in the low-frequency region. The corrosiveness of No.9 sandy soil is weak, and the fitting effect of the equivalent circuit (1) is the best. Regarding R_{ct} and R_s , there may be a nonnegligible interaction between the factors. HCO_3^- has a greater influence on R_{ct} , that is, the corrosiveness of sandy soil, and R_e and R_s are related to the charge storage capacity of the sandy soil. Notably, the initial electrochemical process of No.9 sandy soil is the slowest.

Keywords: orthogonal experiment, sandy soil, EIS, equivalent circuit, corrosiveness

1. INTRODUCTION

Soil is a heterogeneous, multiphase and porous system that can be considered as a corrosive multiphase electrolyte. When metal is in contact with different types of soil, the different interface potentials between the metal and soil cause potential differences on different parts of the metal, which form a loop through the soil to form a corrosion battery, this is a complex process with many influencing factors and can cause serious harm [1]. Chemical corrosion, electrochemical corrosion and stray current interference corrosion are the main forms of corrosion on the outer walls of oil and gas pipelines.

Soil is inherently corrosive and it is related to soil resistivity, soluble salts, water content, pH, microorganisms, oxygen content and their interactions; furthermore, these factors often change over time and space, making the system very complex [2, 3]. Among the above factors, different kinds of soluble salts have different effects on soil corrosiveness. First, soluble salt affects the conductivity of soil. Generally, the higher the salt content is, the lower the soil resistivity, which leads to increased steel corrosion. However, some ions do not increase corrosion. For example, regarding soils rich in limestone and dolomite, the presence of calcium and magnesium ions will deposit lime on the metal surface, which reduces the corrosion rate of metals in the soil [4]. Second, the dissolved salt ions may also participate in the electrochemical reaction process, thereby affecting the corrosiveness of the soil. The salt content also affects the solubility of oxygen in the pore fluid, and nonpolar oxygen molecules have low solubility in salt pore fluid with strong polarity. That is, the higher the salt content is, the lower the oxygen solubility, which weakens the cathodic process of soil corrosion. In addition, acidic media and alkaline media are more corrosive than neutral media. Scholars have found that Cl^- in soil will promote the corrosion of materials, while HCO_3^- and CO_3^{2-} easily promote the formation of an inhibition film on the metal surface that slow down corrosion [5].

Regarding the research methods of soil corrosion, a variety of microscanning techniques (such as open circuit, polarization and electrochemical impedance spectroscopy (EIS) have been used in research of soil corrosion, especially the combination of EIS and polarization curves because more soil corrosion information and corrosion kinetic parameters can be obtained [6, 7]. The EIS test method has gradually been extended to the building materials and geotechnical engineering fields [8-11]. Research on the EIS characteristics of sandy soil is still at the preliminary stage in regard to basic laws and interface theory [12, 13]. The results show that the length and width of the interface zone for a three-phase line have an important influence on the cathodic process and corrosion behavior of metal corrosion [14, 15].

In addition, orthogonal experimental design is another method to study multiple factors and multiple levels; additionally, it is a highly efficient, fast and economical method. According to orthogonality, some representative points, with "uniform, dispersed, neat and comparable" characteristics, are selected from the overall test for testing [16]. To further study the influence of Cl^- , SO_4^{2-} and HCO_3^- on the electrochemical properties of sandy soil, orthogonal experiments on the electrochemical behavior of sandy soil containing Cl^- , SO_4^{2-} and HCO_3^- were conducted, the universality of equivalent circuits was explored, and the influence mechanisms of Cl^- , SO_4^{2-} and HCO_3^- on the electrochemical characteristics of sandy soil were studied along with a statistical range analysis.

2. EXPERIMENTAL METHOD

2.1 Materials

Xiamen ISO standard sand was used in this work, and the silica content was more than 98%. The maximum dry density (ρ_{dmax}) was 1.86 g/cm^3 , the minimum dry density (ρ_{dmin}) was 1.56 g/cm^3 , and the grain size accumulation curve of the standard sand indicated that the standard sand is a good grade of coarse sand (Figure 1). Distilled water was used. The anions were Cl^- , SO_4^{2-} and HCO_3^- (which

significantly affect soil corrosion), and the cation was Na^+ (the most soluble in water). The salts (NaCl , Na_2SO_4 , NaHCO_3) were all analytically pure reagent.

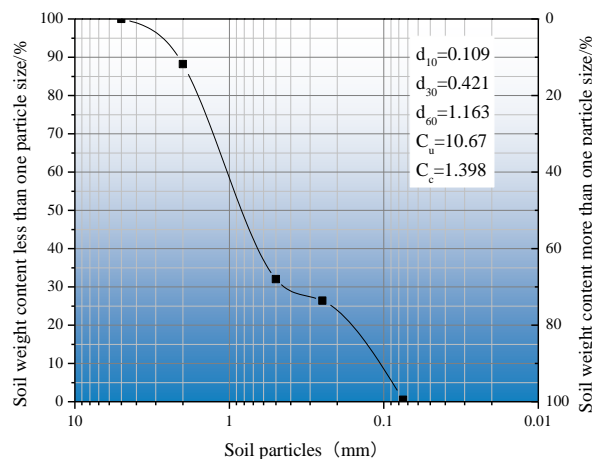


Figure 1. Grain size accumulation curve of the standard sand

A rubber box with an internal volume of $7.07 \times 7.07 \times 7.07 \text{ cm}^3$ was used as the electrolyzer. The amount of standard sand was 500 g, the height was controlled to approximately 6.0 cm under the corresponding medium density, and the water content was 15% when the saturation (S_r) was 71.3%. Weighing is performed on an electronic balance with an accuracy of 0.01.

2.2 Method

The electrochemical impedance spectroscopy test was carried out on the electrochemical workstation (CS350, Wuhan Corrtest Instruments Corp., Ltd.), and the test device was a three-electrode system, as shown in Figure 2.

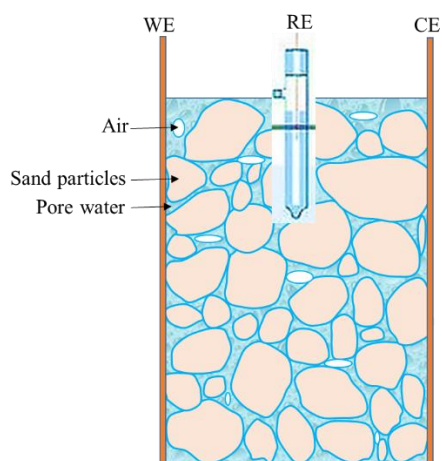


Figure 2. Schematic diagram of test device

Two opposing surfaces of the electrolytic cell were pasted with copper sheet of appropriate size as the working electrode (WE) and the counter electrode (CE). Considering the stability of the test results, the calomel electrode was selected as the reference electrode (RE). The adhesive surfaces of the working electrode and counter electrode were sealed by wax to reduce the influence of the contact area on the test.

To study the influence of three kinds of soluble salts on the electrochemical behavior of sandy soil, the orthogonal group of sandy soil containing a mixture of sodium salts was designed according to the classification of saline soil in the "Code for Investigation of Geotechnical Engineering"[5].

Table 1 is the orthogonal test level table under three factors (Cl^- , SO_4^{2-} and HCO_3^-); moreover, three levels (salt content) were selected for each factor. An L_9 (3^4) orthogonal table was used to arrange the test, and the table header is shown in Table 2. To eliminate the influence of the test sequence on the test results, the test group (sequence as show in Table 3) was designed by IBM SPSS Statistics software.

Table 1. The orthogonal test level table of sandy soil containing mixed soluble sodium salts

Level	C(Cl^-)	C(SO_4^{2-})	C(HCO_3^-)
1	1.00	0.30	0.30
2	5.00	1.00	1.00
3	8.00	2.00	2.00

Note: C is the number of millimoles of ions in 100 g standard sand, the same below.

Table 2. Design of orthogonal test head of sandy soil containing mixed soluble sodium salts

Factor	C(Cl^-)	C(SO_4^{2-})	C(HCO_3^-)	Blank
Column number	1	2	3	4

Table 3. Orthogonal test group of sandy soil containing mixed soluble sodium salts

Samples	C(Cl^-)	C(SO_4^{2-})	C(HCO_3^-)	M/g	Density/($\text{g}\cdot\text{cm}^{-3}$)	Liquid content/%	Salt content/%
No.1	3	2	1	3.17	1.928	15.63	0.63
No.2	1	3	3	2.55	1.926	15.51	0.51
No.3	3	1	3	3.39	1.929	15.68	0.68
No.4	1	2	2	1.42	1.922	15.28	0.28
No.5	2	2	3	3.01	1.927	15.60	0.60
No.6	3	3	2	4.18	1.931	15.84	0.84
No.7	2	3	1	3.01	1.927	15.60	0.60
No.8	2	1	2	2.09	1.924	15.42	0.42
No.9	1	1	1	0.63	1.919	15.13	0.13

Note: Distilled water is 75 g, and M is the total salt content (g).

According to the "Geotechnical Engineering Survey Specification" (GB 50021), the sandy soil used in this test was a weak-saline sandy soil, which is a relatively common saline sandy soil in

engineering. The salt content of the sandy soil decreased in the following order: No. 9 < No. 4 < No. 8 < No. 2 < No. 7 = No. 5 < No. 1 < No. 3 < No. 6. The sands of each group were placed in sealable bags for 24 h to obtain a uniformly mixed sand sample. The electrochemical impedance spectroscopy test conditions were AC amplitude of 10 mV and scanning frequency range of 10^{-2} - 10^5 Hz. The test temperature is approximately 20 °C.

3. RESULTS AND DISCUSSION

3.1 EIS of Sandy Soil Containing Cl^- , SO_4^{2-} and HCO_3^-

The EIS characteristics of each group of sandy soils containing Cl^- , SO_4^{2-} and HCO_3^- are shown in Figure 3. Clearly, the Nyquist diagrams of the sandy soils all present capacitive reactance arcs in the high-frequency region and different diffusion slopes in the low-frequency region. The capacitance arc radii in the Nyquist diagrams of the No. 3, No. 4, No. 8 and No. 9 sandy soils are larger and those of the No. 1 and No. 7 sandy soils are smaller, which may be related to the type and content of ions and the distribution of pore fluid in the sandy soil [17]. The electrochemical impedance spectroscopy of the remaining sandy soils shows their own characteristics under the synergistic effect of the three ions.

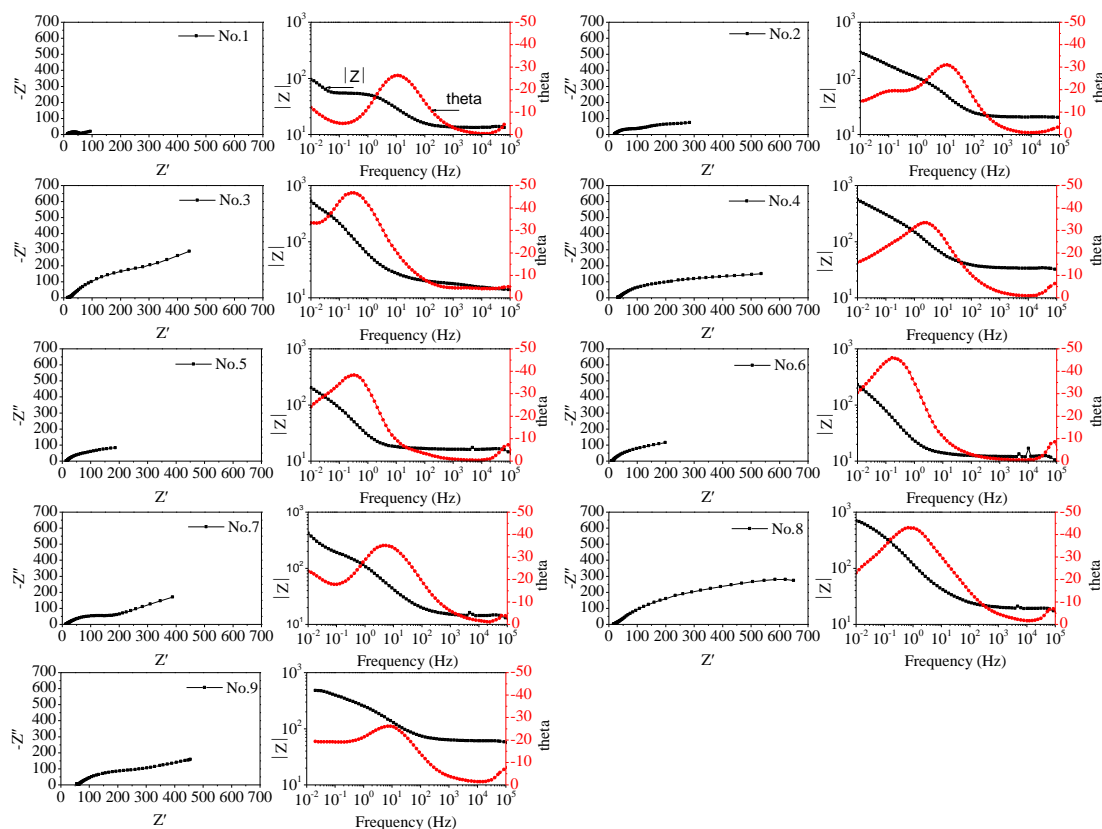


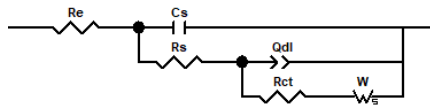
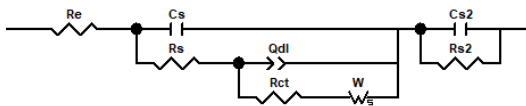

Figure 3. EIS characteristics of sandy soils: Nyquist diagram (Left) and Bode diagram (Right)

Generally, the larger the arc radius of the capacitive impedance is, the more passive the electrochemical reaction process that involves the salt in the sandy soil, which weakens the macroscopic corrosivity to metal [4]. The intersection point of the capacitive resistance arc of the No. 9 sandy soil with the real axis is the farthest to the right, which may be related to it having the lowest salt content; thus, its corrosiveness is weak. The magnitude of the modulus value and the position of the phase angle peak in the Bode diagram also show the corresponding laws, which do not belong to the type that has one time constant. In addition, the curve of the phase angle changing with frequency shows that the pore fluid resistance of the system cannot be ignored [4].

3.2 Equivalent Circuit Fitting of the Impedance Spectroscopy of Sandy Soil

To further study the universal applicability of the equivalent circuit in the sandy soil-electrode system, three equivalent circuits [5] (①, ② and ③), as shown in Table 4) were selected according to the interface structure to fit the impedance spectra of the sandy soil. The fitting software is ZSimDemo3.30. The basic components of the circuits are the resistance of pore fluid (R_e), resistance of the sand layer (R_s), capacitance of the sand layer (C_s), and electric double layer capacitance and Faraday impedance (Q_{dl} ($R_{ct}W$)) formed by contact of the electrode with the pore fluid. Clearly, the fitting effect of equivalent circuit ① is the best, and the fitting results are shown in Figure 4 and Table 5.

Table 4. Equivalent circuit selected for impedance spectrum fitting of sand-system

Number	Equivalent circuit
①	$R(C(R(Q(RW))))$ 
②	$R(C(R(Q(RW))))(CR)$ 
③	$R(Q(RW))(CR)$ 

The results show that with increasing salt content, the R_e tends to decrease overall, and the R_e of the No. 9 sandy soil is the largest. The charge transfer resistance (R_{ct}) reflects the speed of the electrochemical process. The interface in the sandy soil containing more Cl^- (No. 1, No. 3 and No. 6), which has high mobility and is aggressive, fluctuates greatly overall. Thus, the corresponding R_{ct} is unstable, and the sandy soil is more corrosive. R_s and C_s are related to the electric double layer of the interface of the sand particles, indicating that the sandy soil has a certain degree of charge storage capacity [12]. The C_s of the sand systems is on the order of 10^{-4} - 10^{-8} .

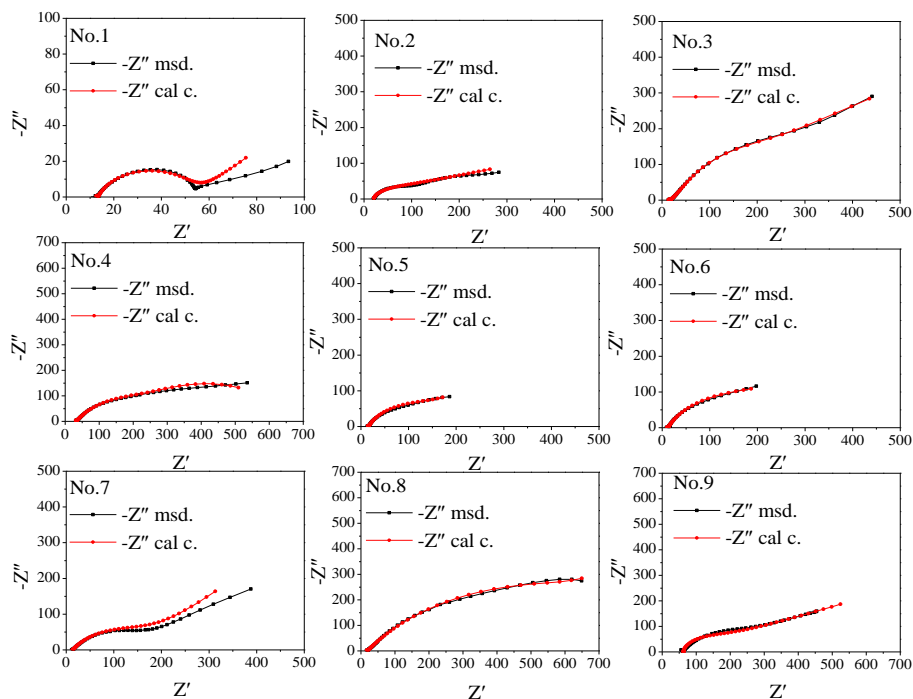


Figure 4. Results of EIS fitting for sandy soils containing Cl^- , SO_4^{2-} and HCO_3^- by equivalent circuit (1)

Table 5. Fitting results for EIS characteristics of sandy soils by equivalent circuit (1)

Samples	Re ($\Omega \cdot \text{cm}^{-2}$)	Qdl		Rct ($\Omega \cdot \text{cm}^{-2}$)	W ($\text{S} \cdot \text{sec}^{-1/2} \cdot \text{cm}^{-2}$)	Cs ($\text{F} \cdot \text{cm}^{-2}$)	Rs ($\Omega \cdot \text{cm}^{-2}$)
		Y ($\text{S} \cdot \text{sec}^{-n} \cdot \text{cm}^{-2}$)	n				
No.1	12.19	1.65E-3	0.76	4.13E1	1.55E-6	1.55E-6	1.21
No.2	20.68	5.91E-3	0.18	5.77E-1	1.59E-4	1.59E-4	6.72E-3
No.3	14.58	5.76E-3	0.65	6.64E2	1.79E-2	1.05E-5	3.92
No.4	22.60	2.10E-3	0.62	4.01E2	2.06E-2	5.34E-8	10.7
No.5	13.02	1.31E-2	0.75	1.59E2	4.60E-7	4.60E-7	3.34
No.6	9.533	1.67E-2	0.74	2.46E2	6.46E-7	6.46E-7	2.91
No.7	12.58	1.91E-3	0.65	1.78E2	9.28E-7	9.28E-7	1.79
No.8	15.77	2.87E-3	0.60	8.92E2	2.38E-2	4.35E-7	3.67
No.9	62.84	3.30E-3	0.24	1.33E-4	2.28E-18	7.28E-5	7.37E-5

The complex three-phase (solid, liquid and gas) coexistence environment makes the capacitance parameter (Y) of the constant phase angle element and diffusion impedance (W) fluctuate greatly, which can reflect the electrochemical process speed in the sandy soil to a certain extent [13]. The parameter n of the constant phase angle element fluctuates between 0.6-0.8, which indicates that the interface capacitance deviates from the ideal capacitance to a certain extent due to the porous structure of the sandy soil at the electrode interface. Generally, the mobility and aggressiveness of Cl^- in sand is greater than other anions, while HCO_3^- contributes to the formation of a passive film on the surface of the electrode, and SO_4^{2-} has a higher charge [4]. The impedance spectroscopy results show the

electrochemical characteristics under the combined effects of the sand-electrode interface structure, the state of the water film and the presence of salt ions.

To verify the reliability of the test data, the K-K (Kramers-Kronig) transformation of the real and imaginary parts is further discussed. The impedance spectrum measurement values and K-K conversion values of each group of sandy soil are shown in Figure 5. The K-K conversion curve is in good agreement with the measurement curve, which shows that the impedance spectrum data are reliable and reasonable [18].

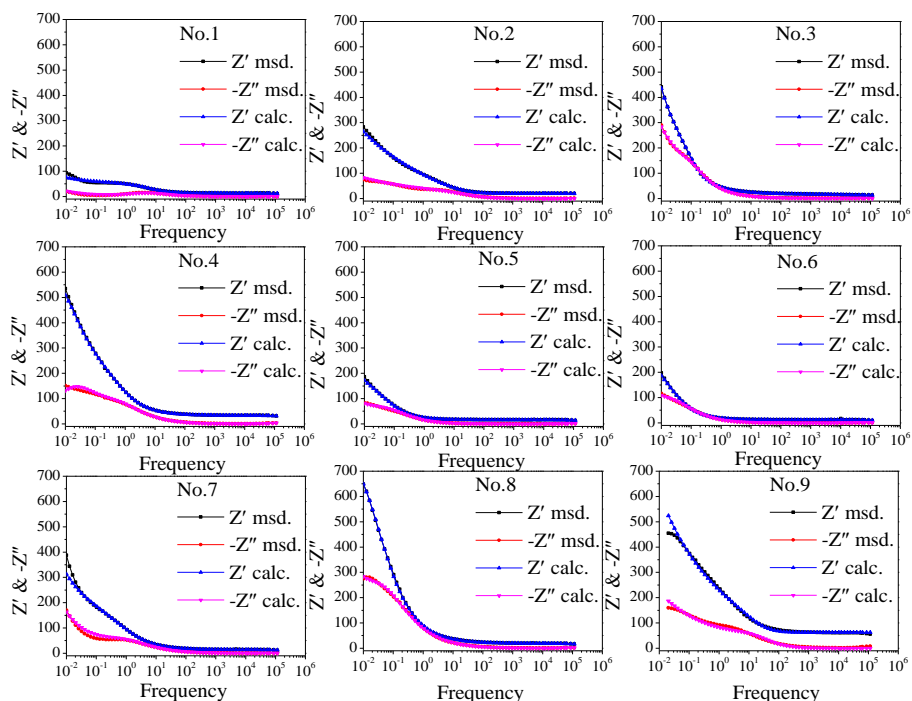


Figure 5. K-K verification of EIS data of sandy soils containing Cl^- , SO_4^{2-} and HCO_3^- under equivalent circuit ①

3.3 Range Analysis of the EIS Results of Sandy Soil

To further analyse the influence of the three ions on the impedance spectroscopy characteristics of sandy soil, a range analysis of the representative parameters in the fitting results was conducted. Orthogonal Design Assistant is an auxiliary software for range analysis. I, II and III are the three level numbers. $I_{i,j,k}$, $II_{i,j,k}$ and $III_{i,j,k}$ are the arithmetic averages of the test results obtained under the corresponding factor levels in any column. $R_{i,j,k}$ are the ranges of each column, which is obtained by $R = \max \{I_{i,j,k}, II_{i,j,k}, III_{i,j,k}\} - \min \{I_{i,j,k}, II_{i,j,k}, III_{i,j,k}\}$.

In this section, the corresponding fitting results of the equivalent circuit ①, with excellent fitting effect, were selected for range analysis, as shown in Table 6. Here, i, j and k represent R_e , R_{ct} and R_s , respectively. The results show that for R_{ct} and R_s , the range of the blank column is larger than the range of other factors, indicating that there may be a nonnegligible interaction between three factors [16].

Table 6. Range analysis of EIS fitting results for sand soil under orthogonal test (equivalent circuit ①)

Samples	C(Cl ⁻)	C(SO ₄ ²⁻)	C(HCO ₃ ⁻)		Re/ Ω·cm ⁻²	Rct/ Ω·cm ⁻²	Rs/ Ω·cm ⁻²
No.9	1	1	1	1	62.84	1.33E-4	7.37E-5
No.4	1	2	2	2	22.60	4.01E2	10.7
No.2	1	3	3	3	20.68	5.77E-1	6.72E-3
No.8	2	1	2	3	15.77	8.92E2	3.67
No.5	2	2	3	1	13.02	1.59E2	3.34
No.7	2	3	1	2	12.58	1.78E2	1.79
No.3	3	1	3	2	14.58	6.64E2	3.92
No.1	3	2	1	3	12.19	4.13E1	1.21
No.6	3	3	2	1	9.533	2.46E2	2.91
Ii	35.37	31.06	29.20	28.46			
IIi	13.79	15.94	15.97	16.59			
IIIi	12.10	14.26	16.09	16.21			
Ri	23.27	16.80	13.24	12.25			
Ij	113.9	518.7	73.10	135.0			
IIj	409.7	200.4	513.0	414.3			
IIIj	317.1	141.5	274.5	311.3			
Rj	275.8	377.1	439.9	279.3			
Ik	3.569	2.530	1.000	2.083			
IIk	2.933	5.083	5.760	5.470			
IIIk	2.680	1.569	2.422	1.629			
Rk	0.889	3.514	4.760	3.841			

In this system, the order of the influence of anions on R_{ct} is $\text{HCO}_3^- > \text{SO}_4^{2-} > \text{Cl}^-$; the order of the influence on R_s is $\text{HCO}_3^- > \text{SO}_4^{2-} > \text{Cl}^-$; and the order of the influence on R_e is $\text{Cl}^- > \text{SO}_4^{2-} > \text{HCO}_3^-$. In the sandy soil with three anions, R_{ct} directly reflects the speed of the initial electrochemical process, and HCO_3^- has a greater influence on the corrosiveness of the sandy soil. R_e and R_s are related to the adsorption double layer of the sand-electrode porous structure under the synergistic effect of the three ions, that is, the charge storage capacity of the sandy soil.

Through the range analysis of the impedance results, the slowest scheme of the electrochemical reaction process can be found. Under this system, the scheme for R_{ct} is the smallest; that is, the slowest initial electrochemical reaction process occurs when the millimoles of Cl^- , SO_4^{2-} and HCO_3^- in 100 g of sand are 1, 2, and 0.3, respectively. Notably, this particular scheme is not in the orthogonal experiment test. Thus, the initial electrochemical process of the No.9 sand in this experiment was the slowest.

4. CONCLUSION

Based on the orthogonal experiment, electrochemical impedance spectroscopy was used to study the characteristics of sandy soils containing Cl^- , SO_4^{2-} and HCO_3^- , and the universality of the equivalent circuit was also studied. The influence of Cl^- , SO_4^{2-} and HCO_3^- on the electrochemical behaviour and corrosivity of sandy soil was studied by range analysis. The following conclusions can be drawn:

(1) The Nyquist diagrams of sandy soils all present capacitive reactance arcs in the high-frequency region and different diffusion slopes in the low-frequency region, which do not belong to the type that has one time constant. For the No.9 sandy soil, the intersection point of its capacitive resistance arc with the real axis is the farthest to the right, and the radius of this capacitance arc is larger; thus, its corrosiveness is weak.

(2) The basic components of the circuits are the resistance of the pore fluid (R_e), resistance of the sand layer (R_s), capacitance of the sand layer (C_s), and electric double layer capacitance and Faraday impedance (Q_{dl} ($R_{ct}W$)) formed by contact of the electrode with the pore fluid. The fitting effect of equivalent circuit ① is the best.

(3) Regarding R_{ct} and R_s , the range of the blank column is larger than the range of other factors, indicating that there may be a nonnegligible interaction between these factors. HCO_3^- has a greater influence on R_{ct} , that is, the corrosiveness of sandy soil, and R_e and R_s are related to the charge storage capacity of the sandy soil. The initial electrochemical process of the No.9 sand in this experiment is the slowest.

ACKNOWLEDGMENTS

The authors would like to express their gratitude to the funding provided by PhD research launch project of Jinzhong University (No. jzxybsjxxm2019019), "1331" Innovation Team of Jinzhong University (jzycxtd2019008), Scientific and technological innovation projects of colleges and universities in Shanxi Province (No. 2020L0588), Opening Project of Sichuan University of Science and Engineering, Material Corrosion and Protection Key Laboratory of Sichuan province (No. 2020CL13), National Natural Science Foundation of China (No. 51208333, No. 41807256), Program for the Outstanding Innovative Teams of Higher Learning Institutions of Shanxi (No.OIT2015), State Key Laboratory of Geomechanics and Geotechnical Engineering, Institute of Rock and Soil Mechanics, Chinese Academy of Sciences (No. Z017003) and Key Laboratory of Ministry of Education for Geomechanics and Embankment Engineering, Hohai University (No. 201702).

References

1. J.Y. Li, C. Men, J.F. Qi, B. Yang and R.M. Liu, *J. Soils Sediments*, 20 (2020) 3204.
2. M. Wasim, S. Shoaib, N. M. Mubarak, Inamuddin and A. M. Asiri, *Environ. Chem. Lett.*, 16 (2018) 861.
3. R.B. Petersen and R.E. Melchers, *Corros. Eng. Sci. Technol.*, 54 (2019) 587.
4. N.M. Lin, L.L. Zhao, Q. Liu, J.J. Zou, R.Z. Xie, S. Yuan, D.L. Li, L.X. Zhang, Z.H. Wang and B. Tang, *J. Phys. Chem. Solids*, 129 (2019) 387.
5. R.Z. Xie, P.J. Han, X.H. Bai, B. He and F.L. Ma, *J. Taiyuan Univ. Technol.*, 50 (2019) 212.
6. I. Ibrahim, M. Meyer, H. Takenouti and B. Tribollet, *J. Brazil Chem. Soc.*, 28 (2017) 1483.
7. X.M. Li and H. Castaneda, *Anti-Corros. Methods Mater.*, 64 (2017) 118.
8. F. Pei, J. Fu, F.Y. Wu, L.J. Wang, X.L. Liu, Z.H. Yin and Z.P. Zhu, *Appl. Mech. Mater.*, 295-298 (2013) 811.
9. H.W. Liu, Y.N. Dai and Y.F. Cheng, *Arabian J. Chem.*, 13 (2020) 3601.
10. J.P. Liu, Y.S. Lu, X.H. Bai, P.J. Han, R.Z. Xie and B. He, *Int. J. Electrochem. Sci.*, 15 (2020) 10694.
11. X.Y. Wang, P.J. Han, X.Q. Dong, X.Y. Li, X.H. Bai, B. He, S.W. Niu and F.N. Sun, *Appl. Sci-Basel*, 10 (2020) 5217.

12. B. He, P.J. Han, L.F. Hou, D.C. Zhang and X.H. Bai, *Eng. Fail. Anal.*, 80 (2017) 325.
13. F.N. Sun, R.Z. Xie, B. He, Z.W. Chen, X.L. Bai and P.J. Han, *Int. J. Electrochem. Sci.*, 16 (2021) 150878.
14. J. Wang and J. Jiang, *Electrochemistry*, 16 (2010) 385.
15. J. Jiang and J. Wang, *Solid State Electrochem.*, 13 (2009) 1723.
16. L. Zhang, X.G. Li and C.W. Du, *J. Iron. Steel Res. Int.*, 16 (2009) 52.
17. F.L. Ma, R.Z. Xie, P.J. Han and X.H. Bai, *Int. J. Electrochem. Sci.*, 13 (2018) 5396.
18. F.G. Liu, Y.H. Zhang, G.J. Ma and C.S. Lu, *Chin. Surf. Eng.*, 22 (2009) 26

© 2021 The Authors. Published by ESG (www.electrochemsci.org). This article is an open access article distributed under the terms and conditions of the Creative Commons Attribution license (<http://creativecommons.org/licenses/by/4.0/>).